DOI: 10.1002/ejic.200701288

From Molecular to Two-Dimensional Anderson Polyoxomolybdate: Synthesis, Crystal Structure, and Thermal Behavior of $[\{Ni(H_2O)_4\}_2\{Ni(OH)_6Mo_6O_{18}\}]\cdot 4H_2O$ and $[Ni(H_2O)_6][Ag_2\{Ni(OH)_6Mo_6O_{18}\}]\cdot 8H_2O$

Feng-Xian Liu,*[a] Catherine Marchal-Roch,[a] Damien Dambournet,[a] Aloïs Acker,[a] Jérome Marrot,[a] and Francis Sécheresse[a]

Keywords: Polyoxometalates / Silver / Nickel / Molybdenum

Two 2D Anderson polyoxomolybdate-based compounds, $[\{Ni(H_2O)_4\}_2\{Ni(OH)_6Mo_6O_{18}\}]\cdot 4H_2O$ (**1**) and $[Ni(H_2O)_6][Ag_2\{Ni(OH)_6Mo_6O_{18}\}]\cdot 8H_2O$ (**2**), were synthesized and characterized by elemental analysis, IR spectroscopy, SEM, and single-crystal XRD. Their thermal behavior was studied by TGA, DSC, XRTD, and IR spectroscopy. Both **1** and **2** are arranged in 2D networks. In **1**, $[Ni(OH)_6Mo_6O_{18}]^{4-}$ Anderson units are covalently linked to each other by two different types of Ni^{2+}, whereas in **2**, the corresponding interactions are ensured exclusively by Ag^+ ions. In addition, all the Ni^{2+} cations in **2** are located in interplanar positions and act selectively as counterions. Upon the addition of silver, the thermal stability of the Anderson anion is increased from 170 °C for pure nickel compound **1** up to 220 °C for mixed silver–nickel **2**. Below 220 °C, **2** exhibits reversible hydration–dehydration processes with preservation of the Anderson anion structure. (© Wiley-VCH Verlag GmbH & Co. KGaA, 69451 Weinheim, Germany, 2008)

Introduction

Polyoxometalate compounds have received much attention due to extreme variabilities in their compositions, molecular architectures, solid-state structures, properties, and applications, particularly in catalysis.[1–3] Recently, Anderson-type heteropolymolybdates $[X(OH)_6Mo_6O_{18}]^{n-}$ have been proposed for precursors of catalysts for hydrodesulfurization (HDS) reactions. It is specifically the case for 6-molybdocobaltate $(NH_4)_3[Co(OH)_6Mo_6O_{18}]$, 6-molybdorhodiumate $(NH_4)_3[Rh(OH)_6Mo_6O_{18}]\cdot 7H_2O$, and 6-molybdoaluminorhodiumate $(NH_4)_3[Rh_xAl_{1-x}(OH)_6Mo_6O_{18}]$, which were studied by Cabello et al.[4,5] and Martin et al, respectively.[6–8]

The $[X(OH)_6Mo_6O_{18}]^{n-}$ Anderson structure is characterized by the presence of a central heteroatom X, generally a octahedral metallic atom surrounded by a crown of six edge-sharing MoO_6 octahedra. The overall wheel adopts a planar configuration.[9,10] Three kinds of oxygen atoms can be distinguished: 12 terminal oxygen atoms O_t, 6 O_b atoms bridging two Mo atoms, and 6 O_c atoms linked to the central heteroatom X and to two Mo atoms of the belt.

Some IR and EXAFS studies have been focused on the structure of Anderson-molybdates, but only a few crystallized phases with X = Cr, Co, Al, Te, Cu, have been characterized by XRD, mainly as ammonium or alkaline salts.[11–17] Recently, the formation of molecular, spiral-shaped, and two-dimensional Anderson inorganic–organic hybrids have been reported.[18–20]

With chromonium, $[(H_2O)_4Ag_3][Cr(OH)_6Mo_6O_{18}]\cdot 3H_2O$ was characterized as an open 3D framework by An et al.,[20] whereas with nickel, the structure of $(NH_4)_4[Ni(OH)_6Mo_6O_{18}]\cdot 4H_2O$ revealed[21] the Anderson units are interlinked by ammonium cations and water molecules.

In this work, we report on the synthesis and crystal structure of two molybdonickelate salts. One is a pure nickel-containing Anderson compound, whereas the other is a mixed Ag–Ni compound. A study of their thermal behaviors by IR spectroscopy, XRD and X-ray thermodiffractometry (XRTD), TGA and DSC was also performed.

Results and Discussion

Crystal Structures

The crystallographic data collection and the structure refinement parameters for $[\{Ni(H_2O)_4\}_2\{Ni(OH)_6Mo_6O_{18}\}]\cdot 4H_2O$ (**1**) and $[Ni(H_2O)_6][Ag_2\{Ni(OH)_6Mo_6O_{18}\}]\cdot 8H_2O$ (**2**) are reported in Table 4.

Crystal Structure of $[\{Ni(H_2O)_4\}_2\{Ni(OH)_6Mo_6O_{18}\}]\cdot 4H_2O$ (1)

The formula deduced from the structure refinement is $H_{30}Mo_6Ni_3O_{36}$. The positions of the hydrogen atoms were located by bond-valence sum calculations. The number of

[a] Institut Lavoisier de Versailles, Université de Versailles Saint-Quentin - UMR CNRS 8180,
45, Avenue des Etats-Unis, 78035 Versailles Cedex, France
Fax: +33-1-39254381
E-mail: Liu@chimie.uvsq.fr

Supporting information for this article is available on the WWW under http://www.eurjic.org or from the author.

water molecules was confirmed by TGA. Selected distances and angles related to the structure are reported in Table 1. Compound **1** exhibits the new two-dimensional structure represented in Figure 1. Anderson units $[Ni(OH)_6Mo_6O_{18}]^{4-}$ are linked by $[Ni(H_2O)_4]^{2+}$ groups to form infinite planes that are self- assembled by hydrogen bonds. The Anderson unit is composed of a central Ni atom sharing edges with six octahedral $MoO_4(OH)_2$ groups to form a hexagonal crown. Six hydroxy groups are coordinated to the central Ni atom. In each $MoO_4(OH)_2$ octahedron, two OH ligands are in *cis* positions, and the octahedron shares two O–OH edges with two neighboring $MoO_4(OH)_2$ moieties and a OH–OH edge with the central $Ni(OH)_6$ group, respectively. Three types of Mo–O distances are observed: long Mo–Oc(H) distances of about 2.2 Å, medium Mo–O distances of about 1.9 Å, and short Mo–O distances of about 1.7 Å for Mo bonded to O_b and O_t. The distance between the central Ni atom and the six O_c oxygen atoms varies from 2.008 to 2.071 Å.

The Anderson units are connected to each other through the Ni2 and Ni3 atoms in a plane perpendicular to the *c* axis as presented in Figure 1. The Ni2 and Ni3 atoms are both six-coordinate, and each nickel atom is bonded to four water molecules and two O_t oxygen atoms pertaining to two perpendicular Anderson units, which thus forms the octahedral $[Ni(H_2O)_4(O_t)_2]$ moiety (O_t–Ni–O_t ≈ 90°). Each

Table 1. Selected bond lengths and angles for **1**.

Bond lengths [Å]					
Mo1–O8	1.707(8)	Mo2–O11	1.707(8)	Mo3–O15	1.721(7)
Mo1–O7	1.722(7)	Mo2–O12	1.724(7)	Mo3–O14	1.737(7)
Mo1–O9	1.907(7)	Mo2–O9	1.934(7)	Mo3–O13	1.925(7)
Mo1–O10	1.979(7)	Mo2–O13	1.951(9)	Mo3–O16	1.957(8)
Mo1–O1	2.227(7)	Mo2–O3	2.227(7)	Mo3–O4	2.176(6)
Mo1–O2	2.227(9)	Mo2–O2	2.232(6)	Mo3–O3	2.232(8)
Mo4–O17	1.718(7)	Mo5–O20	1.704(8)	Mo6–O24	1.708(7)
Mo4–O18	1.719(8)	Mo5–O21	1.718(7)	Mo6–O23	1.712(7)
Mo4–O19	1.922(7)	Mo5–O22	1.937(9)	Mo6–O22	1.926(7)
Mo4–O16	1.947(7)	Mo5–O19	1.939(7)	Mo6–O10	1.955(7)
Mo4–O4	2.225(7)	Mo5–O6	2.220(7)	Mo6–O6	2.197(8)
Mo4–O5	2.226(9)	Mo5–O5	2.237(7)	Mo6–O1	2.212(7)
Ni1–O6	2.008(7)	Ni2–O25	2.010(9)	Ni3–O31	2.017(9)
Ni1–O3	2.020(6)	Ni2–O27	2.053(7)	Ni3–O12	2.036(7)
Ni1–O4	2.022(7)	Ni2–O21	2.059(7)	Ni3–O29	2.039(7)
Ni1–O1	2.028(8)	Ni2–O26	2.061(8)	Ni3–O30	2.047(8)
Ni1–O2	2.048(7)	Ni2–O28	2.065(8)	Ni3–O17	2.073(7)
Ni1–O5	2.071(7)	Ni2–O7	2.070(7)	Ni3–O32	2.099(8)
O1–H1	0.980(7)	O3–H3	0.980(7)	O5–H5	0.980(7)
O2–H2	0.980(7)	O4–H4	0.980(6)	O6–H6	0.979(7)
Bond angles [°]					
O21–Ni2–O7	90.9(3)		O17–Ni3–O12		90.6(3)
O25–Ni2–O7	91.8(3)		O29–Ni3–O12		88.5(3)
O26–Ni2–O7	90.9(3)		O30–Ni3–O12		89.8(3)
O27–Ni2–O7	91.7(3)		O31–Ni3–O12		88.2(3)
O28–Ni2–O7	179.2(3)		O32–Ni3–O12		178.7(3)
O21–Ni2–O26	178.1(3)		O17–Ni3–O30		179.6(3)

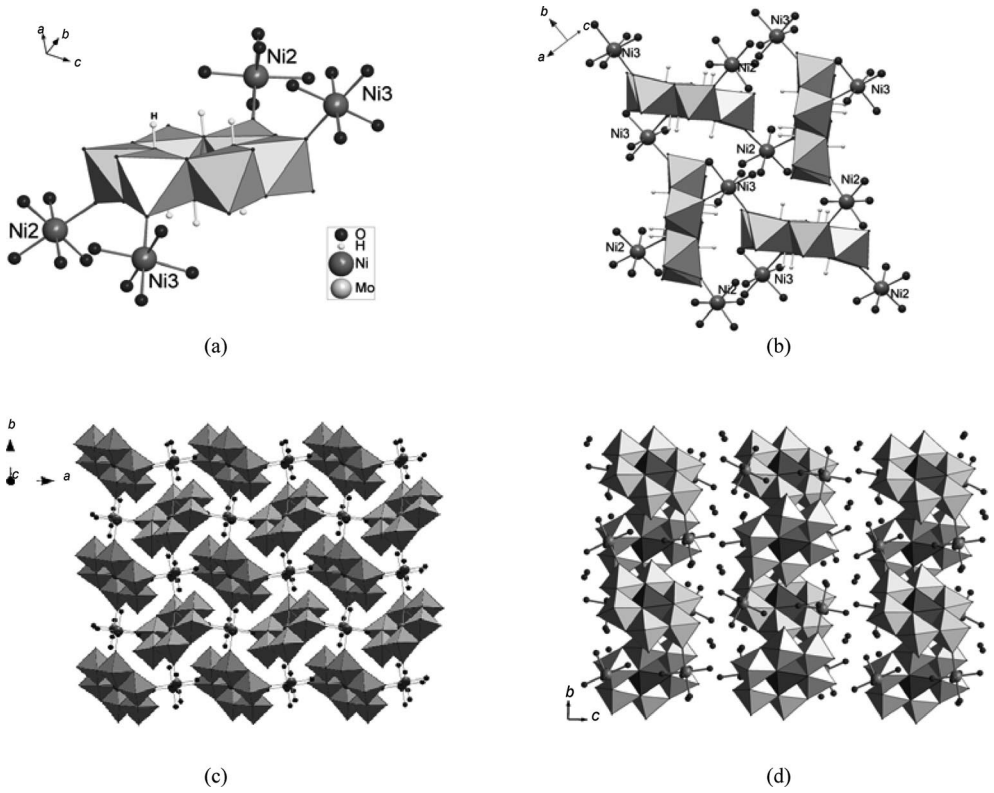

Figure 1. Representation of the two-dimensional structure of $[\{Ni(H_2O)_4\}_2\{Ni(OH)_6Mo_6O_{18}\}]\cdot 4H_2O$ (**1**): (a) connection of an Anderson anion with four Ni; (b) connection of four Anderson anions by Ni atoms; (c) representation of a plane formed by the connection between Anderson anions and Ni atoms; (d) connection of planes ensured by water molecules.

Anderson unit is linked to two Ni2 and two Ni3 atoms through the terminal O7, O21 and O12, O17 oxygen atoms, respectively. One Ni2 and one Ni3 atom are located on one side of hexagonal planar Anderson unit and the two others on the opposite side. Their positions can be exchanged by rotation according to a C_2 axis of the Anderson ring. The Ni2–O_t and Ni3–O_t distances are about 2.0 Å, which is a quite similar value to that of Ni1–O_c(H). A formal plane results from the alternate linking of the Anderson units and Ni atoms. Fourteen-membered rings are formed by four Anderson anions and four Ni atoms without any water included inside (Figure 1b,c). The Anderson units orientate perpendicularly to each other. It can be noted that these Anderson units are also interlinked by hydrogen bonds through the H atoms of the central $Ni(OH)_6$ octahedron and terminal oxygen atoms O_t within two groups: H1–O23 (1.708 Å), H3–O24 (1.765 Å) and H4–O14 (1.683 Å), H6–O15 (1.754 Å), respectively. In each group, two hydrogen atoms are linked to two *cis* O_t atoms of the same $MoO_4(OH)_2$ octahedron. These hydrogen bonds probably play a role in the orientation of the Anderson units. A similar orientation was reported[21] for $(NH_4)_4[NiMo_6O_{24}H_6]\cdot 4H_2O$, where the cohesion between polyanions is ensured only by hydrogen bonds. Here in **1**, the cohesion of the network is not only ensured by Ni^{2+} ions, but also reinforced by hydrogen bonds that impose the perpendicular orientation. Only water molecules (four H_2O per Anderson unit in average) were found between planes (Figure 1d). Consequently, $[\{Ni(H_2O)_4\}_2\{Ni(OH)_6Mo_6O_{18}\}]\cdot 4H_2O$ (**1**) represents a veritable novel 2D-macromolecular structure.

Crystal Structure of $[Ni(H_2O)_6][Ag_2\{Ni(OH)_6MoO_{18}\}]\cdot 8H_2O$ (2)

The empirical formula deduced from the structure refinement is $H_{34}Ag_2Mo_6Ni_2O_{38}$. As for **1**, the number of water molecule and the contents in Ni, Mo, and Ag are confirmed by TGA and elemental analysis, respectively. Some pertinent distances and angles related to the structure are reported in Table 2. This compound exhibits another novel 2D arrangement as represented in Figure 2: the $[Ni(OH)_6Mo_6O_{18}]^{4-}$ Anderson units are linked by Ag^+ ions to form planes that are assembled by weak interactions through octahedral $[Ni(H_2O)_6]^{2+}$ and water molecules. The $[Ni(OH)_6Mo_6O_{18}]^{4-}$ Anderson unit has the same hexagonal structure as **1**. Three kinds of Mo–O distances are observed, and the octahedra containing the central $Ni(OH)_6$ and the $[Ni(H_2O)_6]^{2+}$ counterions are slightly distorted. In Figure 2a are represented the connections of the hexagonal Anderson unit with the Ag^+ cations. Each polyanion is linked to six Ag^+ ions through O_t and O_b atoms. Four Ag atoms are linked to eight O_t atoms among the 12 terminal O_t atoms of one polyanion, whereas the two other Ag atoms are linked to two bridging O_b atoms.

All the Ag atoms are pentacoordinate to three Anderson units (Figure 2b) to form a near square pyramid. Each Ag atom links, in the same basal plane, two O_t atoms of one Anderson unit (d_{Ag-O} = 2.374 and 2.464 Å), one O_b atom of a second Anderson unit (d_{Ag-O} = 2.385 Å), and one O_t atom of a third Anderson unit (d_{Ag-O} = 2.341 Å). Another O_t atom of the third Anderson unit is located at the opposite vertex through a longer distance (d_{Ag-O} = 2.607 Å). The connections between Anderson anions and Ag^+ ions generate an infinite plane parallel to the *ab* plane, which is free of any hydration or coordinated water molecules. All the polyanions orientate towards the same direction (Figure 2c) with only one hydrogen bond between two Anderson units. The plane thus formed is very different from that present in **1**. This can be justified by the strong interaction existing between Ag^+ and three O_t atoms (O1, O2, and O4) of the three Anderson anions (short average bond length of 2.366 Å due to softness of Ag^+). The octahedral $[Ni(H_2O)_6]^{2+}$ group and water molecules are located between these planes (Figure 2d). The comparison of bond length values to literature data permits to postulate that, among the water molecules located in the interplanar space, two of them link two hydroxy groups of a central $Ni(OH)_6$ group through hydrogen bonds [O(H)–O(H_2) distance of 2.783 Å].[21]

The 2D structure of **2** described in this work is totally different from that of the 3D open framework of $[(H_2O)_4Ag_3][Cr(OH)_6Mo_6O_{18}]\cdot 3H_2O$[20] in spite of a similar parallel orientation of the Anderson anions. Among the three types of silver atoms present in $[(H_2O)_4Ag_3][Cr(OH)_6Mo_6O_{18}]\cdot 3H_2O$, two are used to form the plane. All the Ag^+ ions are coordinated not only to terminal and bridging oxygen atoms of the Anderson anion but also to one or two water molecules. Otherwise, in **2**, a weak interaction between an Ag atom and an oxygen atom of a $[Ni(H_2O)_6]$ group is postulated, as the Ag1–O15 distance [2.920(1) Å] is shorter than sum of the van der Waals radii of Ag and O (3.20 Å). The consequence of this interaction is that, as in $[(H_2O)_5Na(C_6NO_2H_4)(C_6NO_2H_5)_3Ag_2]$ and $[Ag_2IMo_6O_{24}(H_2O)_4]\cdot 6.25H_2O$,[23] all the Ag atoms in **2** are six-coordinate in a octahedral geometry, but not five-coordinate as in a square pyramid. The O15 atom behaves as a bridging ligand that links Ni2 on one side and Ag1on another, through an angle of 139.785(4)°. According to this consideration, **2** could be considered a 3D compound.

Table 2. Selected bond lengths and angles for **2**.

Bond lengths [Å]					
Mo1–O1	1.711(1)	Mo2–O8	1.705(2)	Mo3–O12	1.691(2)
Mo1–O2	1.713(2)	Mo2–O7	1.724(1)	Mo3–O11	1.725(2)
Mo1–O4	1.910(2)	Mo2–O3	1.925(2)	Mo3–O9	1.920(1)
Mo1–O3	2.004(3)	Mo2–O9	1.947(2)	Mo3–O4	1.972(2)
Mo1–O6	2.244(3)	Mo2–O10	2.208(2)	Mo3–O5	2.230(3)
Mo1–O5	2.290(2)	Mo2–O6	2.235(3)	Mo3–O10	2.256(2)
Ni1–O10	2.007(3)	Ni2–O13	2.068(2)	Ag1–O2	2.341(2)
Ni1–O10	2.007(3)	Ni2–O13	2.068(2)	Ag1–O1	2.374(0)
Ni1–O6	2.031(2)	Ni2–O14	2.083(2)	Ag1–O4	2.385(2)
Ni1–O6	2.031(2)	Ni2–O14	2.083(2)	Ag1–O7	2.464(3)
Ni1–O5	2.076(2)	Ni2–O15	2.091(2)	Ag1–O11	2.607(2)
Ni1–O5	2.076(2)	Ni2–O15	2.091(2)		
Bond angles [°]					
O1–Ag1–O7		84.8(3)	O2–Ag1–O7		76.4(3)
O1–Ag1–O4		100.9(3)	O2–Ag1–O4		98.0(3)
O1–Ag1–O2		161.0(3)	O4–Ag1–O7		172.8(3)

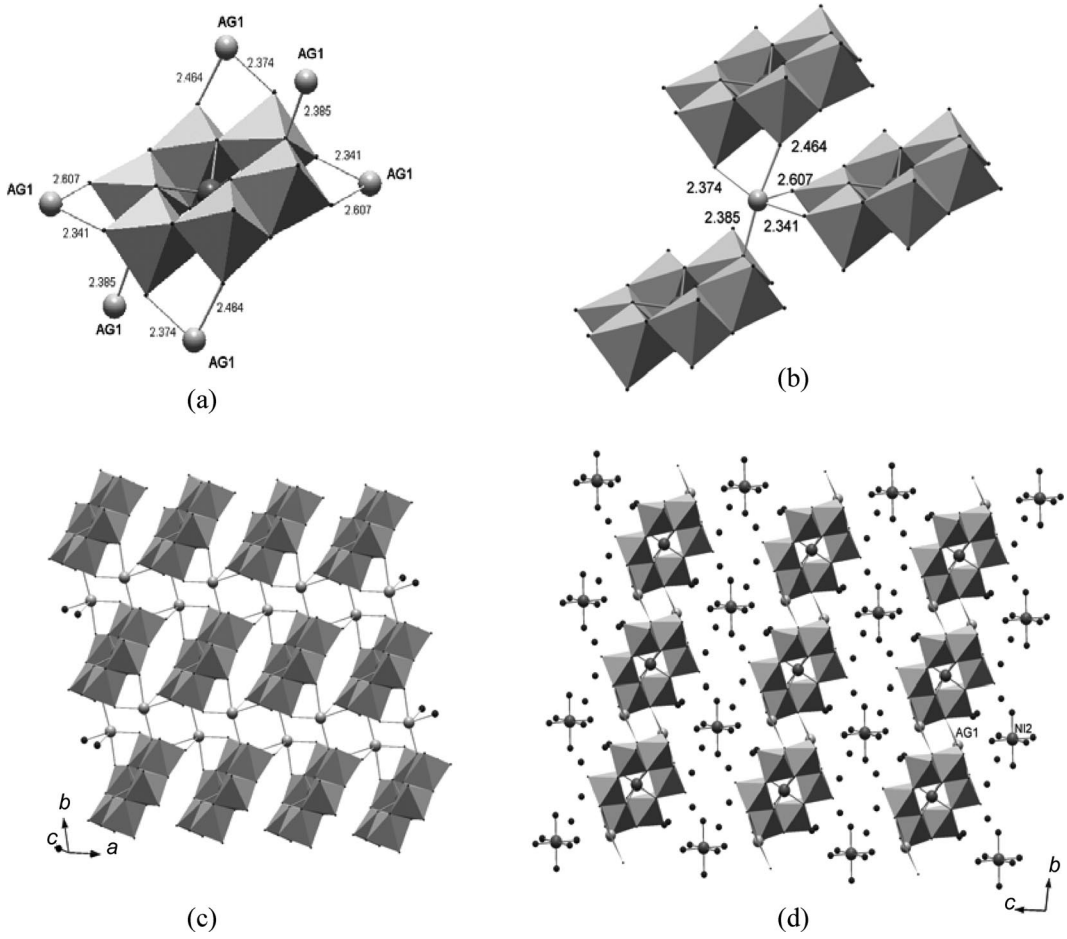

Figure 2. Representation of the 2D structure of **2**: (a) connection of an Anderson anion with six Ag atoms; (b) coordination of Ag by five oxygen atoms of three Anderson anions; (c) view of the plane formed by Anderson anions connected to Ag atoms; (d) view of the layer structure according to the *a* axis; $[Ni(H_2O)_6]^{2+}$ octahedron and water molecules are located in the interplanar space.

Characterizations

Compounds **1** and **2** were characterized at room temperature by SEM, elemental analysis, and IR spectroscopy, and their thermal behaviors were studied by TGA, DSC, IR spectroscopy, and XRTD.

Characterizations at Room Temperature

Elemental analysis results (see Experimental Section) are in agreement with the chemical formula deduced by XRD refinement. SEM images of these two compounds showed two different crystal morphologies (Figure 3): square plane crystals for **1** and stick-like crystals for **2**.

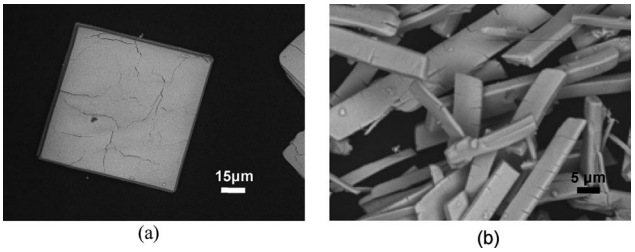

Figure 3. SEM images of (a) **1** (×700) and (b) **2** (×2000).

According to the literature[6,19,24–26] and to the results of thermal treatment experiments, the IR spectra of **1** and **2** exhibit the characteristic bands of the Anderson anion (attributions are given in Table 3). Different vibrational modes can be distinguished: (i) the symmetric and antisymmetric stretching modes of the Mo–O_t group; (ii) the characteristic vibrational mode of the Mo–O_b group, (iii) the characteristic vibrational mode of the Mo–O_c group, and (iv) lattice modes and coupling modes of the Anderson structure.

Table 3. IR spectroscopic data for **1** and **2**.[a]

$\tilde{\nu}$ for **1** [cm^{-1}]	$\tilde{\nu}$ for **2** [cm^{-1}]	Assignment
945 (sh.)	928 (s)	ν_s(Mo–O_t)
930 (s)	915 (sh.)	ν_{as}(Mo–O_t)
900 (vs)	880 (vs)	ν_{as}(Mo–O_t)
789 (w)		
633 (vs)	635 (vs)	ν(Mo–O_b)
573 (s)	582 (sh.)	ν(Mo–O_b)
496 (sh.)	480 (w)	ν(Mo–O_c)
398 (m)	387 (m)	ν(Mo–O_c)
322 (w)	313 (w)	lattice modes

[a] vs: very strong, s: strong, m: medium, w: weak, sh.: shoulder.

The frequencies of the symmetric and antisymmetric vibrations of the Mo–O_t bond depend on the nature of the metallic cation bridged to the O_t atoms of the polyanion. When the Anderson units are linked by Ni^{2+} as in **1**, ν_s(Mo–O_t) and ν_{as}(Mo–O_t) are located at 945, 930, and 900 cm^{-1}, whereas when the Anderson anions are interlinked by Ag^+ ions the band positions decrease to 928, 915, and 880 cm^{-1}. This frequency decrease indicates a weakening of the Mo–O_t bond strength and allows the supposition that the interaction between the Ag^+ ions and the Anderson anion is stronger than that with nickel. The frequencies of other vibrational modes are also perturbed, particularly the relative intensity of the Mo–O_b bands: in **1**, the two ν(Mo–O_b) bands observed at 573 cm^{-1} and 633 cm^{-1} have almost the same intensity, whereas for **2**, the ν(Mo–O_b) band at 582 cm^{-1} is so weak that it is observed as a shoulder among the other ν(Mo–O_b) band at 635 cm^{-1}.

Some studies claimed that there was no visible influence of the nature of the heteroatom X on the Mo–O frequencies of the Anderson unit.[24,27] More recently, a detailed study was reported[26] by Botto et al. on $(NH_4)_3[X^{III}(OH)_6Mo_6O_{18}]$, which showed that Mo–$O_t$ frequencies are the most affected by changes in X. A slight shift to higher frequencies was observed when the size of X was increased in the isomorphism series. Nevertheless, to the best of our knowledge, no decisive IR studies about the influence of the nature of the cation bridging Anderson units on the Mo–O bands have been reported. Here, it appeared that the frequencies of the Mo–O vibrational bands and the relative intensities of the two Mo–O_b bands and the Mo–O_t band are considerably affected by the nature of the metallic atoms, Ni and Ag, bridging the Anderson units.

Thermal Behavior

The thermal behavior of some Anderson-type heteropolymolybdates has been published and analyzed by several research groups,[5,25,28–30] but nothing is reported on the 6-molybdonickel Anderson structure. The TGA and DSC plots of compounds **1** and **2** are shown in Figure 4. The evolution of the solid and specifically of the Anderson anion structure was analyzed by XRTD (Figures 5 and 6) and/or powder XRD and IR spectroscopy.

Compound 1

The TGA plot of **1**, represented in Figure 4a exhibits three weight losses. The first one, between 25 and 100 °C, is attributed to the evolution of four water molecules located between the planes. The second one, between 100 and 180 °C, is attributed to the loss of four water molecules attached to Ni2 and Ni3. Finally, the third one, between 180 and 450 °C, corresponds to the evolution of four other coordinated water molecules and three structure water molecules originating from six OH groups coordinated to the central Ni1 heteroatom, which is indicative of decomposition of the Anderson structure. The variations in the XRTD patterns of **1** are shown in Figure 5. The monoclinic phase of **1** is maintained up to 60 °C and then disappears at 80 °C, whereas another novel phase is observed at 120 °C after the loss of interplanar water. The departure of half of the coordinated water molecules induces a complete amorphization of the solid at about 180 °C. Crystallized oxide phases appear at 440 °C, identified as MoO_3 and $NiMoO_4$, which shows that the Anderson structure has been completely destroyed.

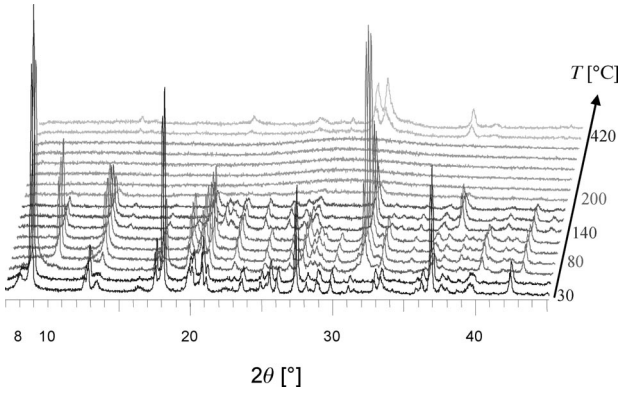

Figure 5. Evolution of the X-ray diffraction pattern of **1** in static air at temperatures of 30, 40, 60, 80, 100, 120, 140, 160, 180, 200, 240, 280, 320, 360, 400, 420, and 440 °C.

The thermal treatment of **1** at 100, 170, 220, and 300 °C was performed in air. The initial light-green color of **1** changes progressively to yellow at 170 °C and then to orange at 300 °C. The IR spectra reveal that the polyanion structure is conserved up to 170 °C but a partial decompo-

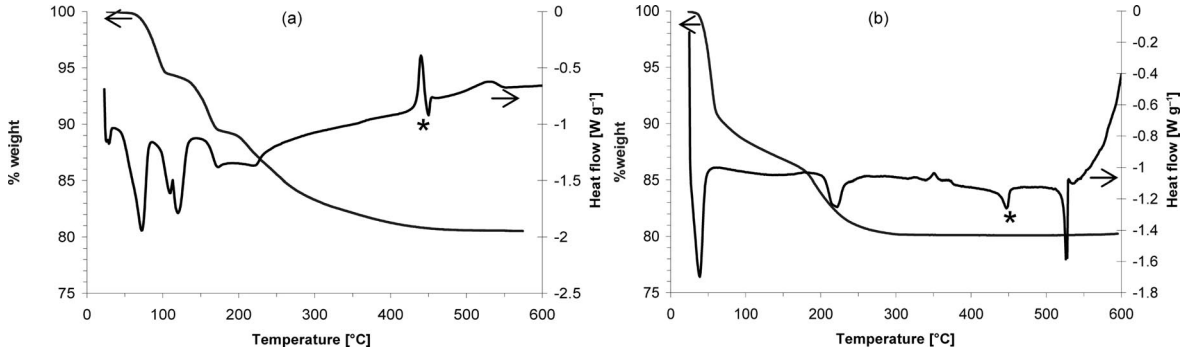

Figure 4. TGA and DSC curves of (a) **1** and (b) **2**; * peak due to DSC apparatus.

sition is observed after 2 h of treatment at 170 °C. The total decomposition is complete at 220 °C. The DSC results are in agreement with TGA, XRTD, and IR studies. The loss of the water molecules located in interplanar positions and half of the water ligands are accompanied with endothermic features at 75, 110, and 120 °C. According to TGA, the departure of the remaining half of the water ligands cannot be distinguished from that of the structure water, but two large endothermic peaks, in spite of their partial superimposition, are observed with higher intensity at about 170 and 230 °C. By considering the XRTD and IR studies, it can be assumed that the endothermic peak near 170 °C corresponds to the evolution of the remaining coordinated water molecules, and the peak at 230 °C corresponds to the loss of the structure water molecules, because the Anderson structure is conserved after treatment for 2 h at 170 °C and then decomposes above 170 °C. Finally the exothermic peak at 440 °C corresponds to the crystallization of the formed oxides and confirms the MoO_3 and $NiMoO_4$ oxide phases observed by XRTD. These data permit to summarize the thermal behavior of **1** by the diagram represented in Scheme 1.

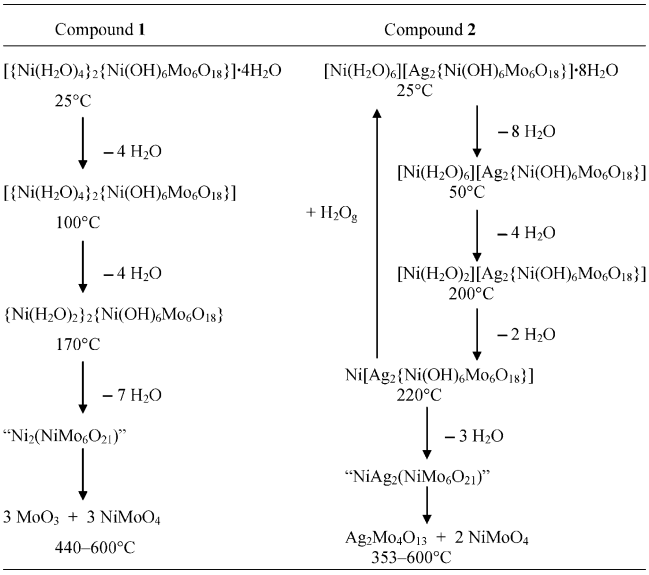

Scheme 1. Thermal behavior of compounds **1** and **2**.

Compound 2

The TGA plot of **2**, given in Figure 4b, exhibits four domains corresponding to a total loss of 17 water molecules. At the beginning of the process, an abrupt loss is observed before 60 °C, which corresponds to the departure of eight hydration water molecules. It is then followed up to 175 °C by a broad loss attributed to the evolution of four water molecules coordinated to Ni2. The third domain, between 175 and 300 °C corresponds to the departure of the two remaining coordinated water molecules and to three structure water molecules. Finally, nothing is observed from 300 °C up to 600 °C.

Three endothermic peaks are associated to the three weight losses. The abrupt departure of the eight hydrated water molecules is characterized by a narrow and intense endothermic peak at 40 °C, whereas the broad departure of the first four coordinated water molecules corresponds to a wide endothermic peak between 65 and 185 °C. The last departure of the mixed coordination/structure water molecules is coupled to the DSC endothermic peak at about 223 °C. After careful examination, this peak was deconvoluted as the superimposition of two weak peaks at 220 and 230 °C, which illustrates the difficulty in separating the departure of the two last coordinated water molecules from structure water. Two other peaks are present in the DSC plot: a weak exothermic one at 353 °C and a narrow intense endothermic one at 525 °C. The peak at 353 °C was attributed to the crystallization of $Ag_2Mo_4O_{13}$ and $NiMoO_4$, which were both identified by powder XRD of **2** after thermal treatment. The melting point of $Ag_2Mo_4O_{13}$ is characterized by the narrow strong endothermic peak at 525 °C.

The infrared spectra of **2** monitored after thermal treatment in air revealed that the Mo–O bands, characteristic of the Anderson structure, are present up to 220 °C. The frequency associated to the $Mo–O_t$ vibration is not temperature dependent in the domain from 25 to 220 °C, whereas that of the bridging $Mo–O_b$ varies from 632 to 619 cm^{-1} as the temperature is increased from 100 to 200 °C. An increase in frequency of the $Mo–O_c$ vibration, from 387 to 396 cm^{-1}, is also observed after thermal treatment at 50 °C. This increase may be explained by a strengthening of the $Mo–O_c$ bond, probably due to a break of the hydrogen bonds after the loss of eight crystallization water molecules at 50 °C. Four water molecules coordinated to Ni2 were lost after a thermal treatment at 200 °C, which resulted in a decrease in the $Mo–O_b$ frequency in the range 100–200 °C related to the $Mo–O_b$ bond weakening. Thus, it can be assumed that after the partial loss of coordinated water, the nickel atom probably sticks to the Anderson anions through O_b oxygen atoms, which results in weakening of the $Mo–O_b$ bond.

A similar evolution of the crystallized phases was evidenced by XRTD patterns of **2** (see Figure 6). Three different phases were observed from 30 to 180 °C, which corresponds to the loss of interlayered water molecules. The departure of coordinated water molecules resulted in an

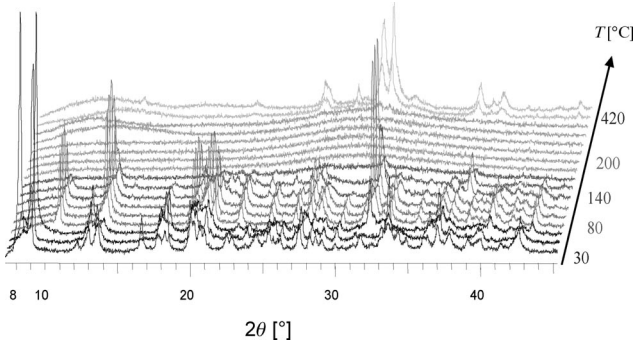

Figure 6. Evolution of the X-ray diffraction pattern of **2** in static air at temperatures of 30, 40, 60, 80, 100, 120, 140, 160, 180, 200, 240, 280, 320, 360, 400, 420, and 440 °C.

amorphous solid at 200 °C. The molybdate phases were formed at 420 °C, a temperature where MoO_3 is not present. This confirms both the powder XRD results obtained after TGA at 600 °C and the destruction of the Anderson structure characterized by IR.

A study of the samples, placed under a water vapor atmosphere after thermal treatment at 220 °C and below, showed that the solid recovered their initial color and powder XRD of the fresh sample except a slight intensity decrease. This implies that the dehydration is reversible up to 220 °C and the Anderson structure is maintained. The thermal behavior of **1** and **2** is summarized in Scheme 1.

Conclusions

Two novel 2D compounds $[\{Ni(H_2O)_4\}_2\{Ni(OH)_6Mo_6O_{18}\}]\cdot 4H_2O$ (**1**) and $[Ni(H_2O)_6][Ag_2\{Ni(OH)_6Mo_6O_{18}\}]\cdot 8H_2O$ (**2**) were prepared from molecular Anderson-type polyoxomolybdate precursors, by insertion of Ni^{2+} and Ag^+ ions. In **1**, Ni^{2+} cations interlink the Anderson anions to form a 2D framework. In **2**, which contains both Ag^+ and Ni^{2+} ions, only the Ag^+ ions directly connect the Anderson anions to form infinite planes. This means that Ag^+ is a more efficient coordination center than Ni^{2+} towards the Anderson anion. This may be explained by the larger softness and the more flexible radius of silver. The study of the thermal behavior of **1** and **2** by IR spectroscopy showed that the polyanions interlinked by Ag^+ conserve their structure up to 220 °C and those interlinked by Ni^{2+} are conserved only up to 170 °C, which indicates a stronger interaction with Ag^+. Furthermore, the hydration–dehydration process for **2** is reversible below 220 °C. Relative to the ammonium salt, compounds **1** and **2** permit an increase in the Ni/Mo ratio from 1:6 to 1:2 and 1:3, respectively. The Anderson-anion structure is conserved up to 170 or 220 °C, and no crystallized phase was observed between 180 and 420 °C. These behaviors could be interesting for the preparation of HDS catalysts, particularly to vary the composition and favor a good dispersion.

Experimental Section

Materials and Synthesis: All chemicals were of reagent grade and used as purchased without further purification. Water used in the reactions was permuted water. $H_3PMo_{12}O_{40}$ acid was synthesized, purified by crystallization, and checked by IR spectroscopy and TGA analysis.[31]

$[\{Ni(H_2O)_4\}_2\{Ni(OH)_6Mo_6O_{18}\}]\cdot 4H_2O$ (1): $Ni(CH_3COO)_2\cdot 4H_2O$ (2.2 g, 8.75 mmol) was added to a solution of $H_3PMo_{12}O_{40}$ prepared by dissolving $H_3PMo_{12}O_{40}\cdot 29H_2O$ (3 g, 1.25 mmol) in water (20 mL). Light-green crystals were obtained at room temperature after two weeks. Yield: 0.6 g (20% based on Mo). $H_{30}Mo_6Ni_3O_{36}$ (1357.91): calcd. Mo 42.64, Ni 13.04; found Mo 40.92, Ni 12.16. Atomic ratio: calcd. Mo/Ni 2.00; found Mo/Ni 2.05.

$[Ni(H_2O)_6][Ag_2\{Ni(OH)_6Mo_6O_{18}\}]\cdot 8H_2O$ (2): $Ni(CH_3COO)_2\cdot 4H_2O$ (2.48 g, 10 mmol) was added to a solution of $H_3PMo_{12}O_{40}$ obtained by dissolving $H_3PMo_{12}O_{40}\cdot 29H_2O$ (6 g, 2.5 mmol) in water (38 mL). After addition of Ag_2CO_3 (1.38 g, 5 mmol) and heating to 35 °C to dissolve Ag_2CO_3, the mixture was maintained whilst stirring at 35 °C over 2 h. A solid was eliminated by filtration and identified as silver heptamolybdate. The filtrate was kept at room temperature and thin needle-shaped green crystals were recovered after two weeks. Yield: 0.14 g (2% based on Mo). $H_{34}Ag_2Mo_6Ni_2O_{38}$ (1550.99): calcd. Mo 37.11, Ag 13.90, Ni 7.56; found Mo 35.98, Ag 13.11, Ni 7.15. Atomic ratio: calcd. Mo/Ag 3.00, Mo/Ni 3.00, Ni/Ag 1.00; found Mo/Ag 3.08, Mo/Ni 3.07, Ni/Ag 1.00.

Crystal-Structure Analysis: A single crystal of **1**, $0.08 \times 0.08 \times 0.01$ mm, was glued on a glass fiber for the structure determination by X-ray diffraction. X-ray intensity data were collected at 263 K with a Bruker-Nonius X8-APEX2 CCD area-detector diffractometer by using Mo-K_α radiation (λ = 0.71073 Å). Three sets of narrow data frames were collected at different values of θ, for two and one initial values of ϕ and ω, respectively, by using 0.5° increments of ϕ or ω. Data reduction was accomplished by using SAINT V7.03.[32] The substantial redundancy in data allowed a semiempirical absorption correction (SADABS V2.10)[32a] to be applied, on the basis of multiple measurements of equivalent reflections. The structure was solved by direct methods, developed by successive difference Fourier syntheses, and refined by full-matrix least-squares on all F^2 data by using SHELXTL V6.14.[32b] Hydrogen atoms were included in calculated positions and allowed to ride on their parent atoms.

A single crystal of **2** of dimensions $0.12 \times 0.04 \times 0.01$ mm was carefully selected and glued on a glass fiber. X-ray data were recorded at room temperature with a Siemens SMART 1K three-circle diffractometer equipped with a CCD two-dimensional detector by using Mo-K_α radiation (λ = 0.71073 Å). Slightly more than one hemisphere of data was recorded. The frames were recorded with a scan width of 0.3° in ω and an exposure time of 120 s. An empirical absorption correction was applied by using the SADABS program based on the method of Blessing. The structure was solved by direct methods and refined by full-matrix least-squares by using the SHELX-TL package. Hydrogen atoms were placed in calculated positions and allowed to ride on their parent atoms.

Crystallographic and structure refinement data for **1** and **2** are collected in Table 4. Further details of the crystal-structure investigations may be obtained from the Fachinformationszentrum Karlsruhe, 76344 Eggenstein-Leopoldshafen, Germany, on quoting the depository number(s) CSD-418856 and -418857.

Table 4. Crystallographic and structure refinement data for **1** and **2**.

	Compound **1**	Compound **2**
Empirical formula	$H_{30}Mo_6Ni_3O_{36}$	$H_{34}Ag_2Mo_6Ni_2O_{38}$
Crystal symmetry	monoclinic	triclinic
Space group	$P1\ 2_1/c\ 1$(No. 14)	$P\bar{1}$ (No. 2)
Unit cell		
a [Å]	11.528(2)	7.1251(7)
b [Å]	11.427(2)	9.723(1)
c [Å]	22.644(3)	12.674(1)
α [°]	90.00	92.314(2)
β [°]	98.081(7)	99.106(2)
Volume [Å^3]	2953.3(6)	830.3(2)
Z	4	1
$\rho_{calcd.}$ [g cm^{-3}]	3.054	3.101
λ [Å]	0.71073	0.71073
GOF	1.113	0.937
Final R_1 [$I > 2\sigma(I)$]	0.0544	0.0608
Final wR_2 [$I > 2\sigma(I)$]	0.1414	0.1137

Characterization and Thermal Treatment: The morphology of the crystals was observed by scanning electron microscopy (SEM) by using a JEOL JSM-5800LV microscope. X-ray thermodiffractometry (XRTD) was performed in air in an Anton Paar HTK16 high-temperature device of a Siemens D5000 diffractometer (θ-θ mode) by using Co-K_α radiation (λ = 1.7903 Å), and equipped with an M Braun linear position sensitive detector (PSD). Patterns were recorded from 30 to 600 °C every 20 °C above 40 °C, with a temperature slope of 1.8 °C min^{-1}. The temperature was kept 2 min before measurements; each data collection lasted 570 s.

Thermogravimetry measurements (TGA) were carried out in air flow (60 mL min^{-1}) with a Perkin–Elmer electrobalance TGA-7 at a heating rate of 5 °C min^{-1} up to 600 °C. Differential scanning calorimetry (DSC) was performed in air flow (60 mL min^{-1}) with a TA Instruments DSC 2010 at a heating rate of 5 °C min^{-1} up to 600 °C. Infrared spectra of KBr pellets were recorded with an FTIR Nicolet Magna 550 apparatus.

In order to study their thermal behavior, **1** and **2** were treated in air at different temperatures over 2 h before their IR spectra and powder X-ray diffraction patterns were recorded.

Supporting Information (see footnote on the first page of this article): IR spectra of **1** and **2** after thermal treatment; powder X-ray diffraction patterns for the reversible hydration of **2**.

Acknowledgments

This work is supported by the Centre National de Recherche Scientifique (CNRS) and the Direction Générale de la Recherche Scientifique (DGRST).

[1] M. Misono, *Chem. Commun.* **2001**, 1141.
[2] I. V Kozhevnikov in *Catalyst for Fine Chemical Synthesis – Catalysis by Polyoxometalates*, John Wiley and Sons, **2002**, p. 117.
[3] C. L. Hill, "*Polyoxometalate: Reactivity*" in *Comprehensive Coordination Chemistry II* (Ed.: A. G. Wedd), Elsevier, Oxford, **2004**, vol. 4, pp. 679–759.
[4] C. I. Cabello, I. L. Botto, H. J. Thomas, *Appl. Catal., A* **2000**, *197*, 79–86.
[5] C. I. Cabello, M. Munoz, I. L. Botto, E. Payen, *Thermochim. Acta* **2006**, *447*, 22–29.
[6] C. Martin, C. Lamonier, M. Fournier, O. Mentré, V. Harlé, D. Guillaume, E. Payen, *Inorg. Chem.* **2004**, *43*, 4636–4644.
[7] E. Payen, G. Plazenet, C. Martin, C. Lamonier, J. Lynch, V. Harlé, *Studies Surface Science Catal.* **2002**, *143*, 141–148.
[8] G. Plazenet, E. Payen, J. Lynch, B. Rebours, *J. Phys. Chem. B* **2002**, *106*, 7013–7028.
[9] M. T. Pope, *Heteropoly and Isopoly Oxometalates*, Springer, Berlin, **1983**.
[10] K. Nomiya, T. Takahashi, T. Shirai, M. Miwa, *Polyhedron* **1987**, *6*, 213–218.
[11] H. T. Evans Jr., *J. Am. Chem. Soc.* **1967**, *90*, 3275.
[12] H. T. Evans Jr., *Acta Crystallogr., Sect. B* **1974**, *30*, 2095.
[13] A. Perloff, *Inorg. Chem.* **1970**, *9*, 2228.
[14] L. Lukasz Lebioda, M. Ciechanowicz-Rutkowska, L. C. W. Baker, J. Grochowski, *Acta Crystallogr., Sect. B* **1980**, *36*, 2530.
[15] H. Kondo, A. Kobayashi, Y. Sasaki, *Acta Crystallogr.*, Sect. B **1980**, *36*, 661.
[16] K. J. Schmidt, G. J. Schrobilgen, J. F. Sawyer, *Acta Crystallogr.*, Sect. C **1986**, *42*, 1115.
[17] F. Ito, T. Ozeki, H. Ichida, H. Miyamae, Y. Sasaki, *Acta Crystallogr.*, Sect. C **1989**, *45*, 946.
[18] S. Manikumari, V. Shivaiah, S. K. Das, *Inorg. Chem.* **2003**, *42*, 6604–6606.
[19] B. Hasenknopf, R. Delmont, P. Herson, P. P. Gouzerh, *Eur. J. Inorg. Chem.* **2002**, 1081–1087.
[20] H. An, Y. Li, D. Xiao, E. Wang, C. Sun, *Cryst. Growth & Des.* **2006**, *6*, 1107–1112.
[21] U. Lee, H.-C. Joo, J.-S. Kwon, *Acta Crystallogr.*, Sect. E **2002**, *58*, 16–18.
[22] S. Manikumari, V. Shivaiah, S. K. Das, *Inorg. Chem* **2002**, *41*, 6953–6955, and ref. herein.
[23] H. An, Y. Li, E. Wang, D. Xiao, C. Sun, L. Xu, *Inorg. Chem.* **2005**, *44*, 6062–6070.
[24] K. Nomiya, T. Takahashi, T. Shirai, M. Miwa, *Polyhedron* **1987**, *6*, 213–218.
[25] I. L. Botto, C. I. Cabello, H. J. Thomas, *Mater. Chem. Phys.* **1997**, *47*, 37–45.
[26] I. L. Botto, A. C. Garcia, H. J. Thomas, *J. Phys. Chem. Solids* **1992**, *53*, 1075–1080.
[27] D. Mesure, P. Chaquin, C. Louis, M. Che, M. Fournier, *J. Catal.* **1989**,*119*, 415.
[28] A. La Ginestra, M. Seta, *Ric. Sci.* **1967**, *37*, 287.
[29] A. La Ginestra, R. Cerri, *Gazz. Chim. Ital.* **1965**, *95*, 26.
[30] C. I. Cabello, I. L. Botto, H. J. Thomas, *Thermochim. Acta* **1994**, *232*, 183–193.
[31] C. Rocchiccioli-Deltcheff, R. Thouvenot, R. Franck, *Inorg. Chem.* **1983**, *22*, 207.
[32] a) *APEX2* (version 1.0–8), Bruker AXS, Madison, **2003**; b) *SHELXTL* (version 6.14), Bruker AXS, Madison, **2001**.

Received: November 29, 2007
Published Online: March 20, 2008

